Journal of Electrical Engineering & Technology Vol. 7, No. 2, pp. 207~211, 2012 **207**
http://dx.doi.org/10.5370/JEET.2012.7.2.207

Preparation and Characteristics of $Li_4Ti_5O_{12}$ Anode Material for Hybrid Supercapacitor

Byung Gwan Lee* and Jung Rag Yoon†

Abstract – Spinel-$Li_4Ti_5O_{12}$ was successfully synthesized by a solid-phase method at 800, 850, and 900℃ according to the $Li_4Ti_5O_{12}$ cubic spinel phase structure. To achieve higher EDLC energy density with the $Li_4Ti_5O_{12}$, the negative electrode of the hybrid supercapacitor was studied in this work. The electrochemical performances of the hybrid supercapacitor and EDLC were characterized by constant current discharge curves, c-rate, and cycle performance testing. The capacitance (1st cycle) of the hybrid supercapacitor and EDLC was 209 and 109 F, respectively, which is higher than EDLC. The capacitance of the hybrid supercapacitor decreases from 209 F to 101 F after 20 cycles when discharged at several specific current densities ranging from 1 to 10 A. In contrast, capacitance of the EDLC hardly decreases after 20 cycles. Results show that hybrid supercapacitor benefits from the high rate capability of supercapacitor and high capacity of the battery. Findings also prove that the hybrid supercapacitor is an energy storage device where the supercapacitor and the Li ion secondary battery coexist in one cell system.

Keywords: $Li_4Ti_5O_{12}$, LTO, Lithium titanate, Hybrid supercapacitor, Hybrid capacitor

1. Introduction

Spinel-$Li_4Ti_5O_{12}$ has attracted attention as a promising anode material because of the near-zero change in the unit cell volume during charge and discharge. Spinel-$Li_4Ti_5O_{12}$ can accommodate lithium ions during discharge, resulting in a structural transition from spinel-$Li_4Ti_5O_{12}$ to rock-salt phase $Li_7Ti_5O_{12}$ without noticeable changes in the lattice parameter. During cycling processes, lithium insertion into the spinel-$Li_4Ti_5O_{12}$ relocates lithium from tetrahedral 8a sites to the octahedral 16c sites with the formation of a rock-salt $Li_7Ti_5O_{12}$, which may be rendered as

$$Li_4Ti_5O_{12} + 3Li^+ + 3e \leftrightarrow Li_7Ti_5O_{12},\ E= 1.5V$$

These characteristics ensure long life cycle and excellent cycle performance. The $Li_4Ti_5O_{12}$ inserts three lithium ions per formula unit, with a theoretical capacity of 175 mAhg-1, showing a voltage flat at 1.55 V versus a lithium electrode [1]. However, these are the characteristics of insulating materials. The low conductivity of $Li_4Ti_5O_{12}$ leads to initial capacity loss and poor rate capability. To improve the low conductivity, synthesizing the nanosized particles via various methods is proposed. Small-sized particle will obviously shorten the Li^+ diffusion path and broaden the electrode/electrolyte contact surface [2]. Various synthesis methods are available for the fabrication of $Li_4Ti_5O_{12}$ such as, solid-state reaction [3-5], sol–gel [6-8], hydrothermal [9], spray pyrolysis [10], molten salt [11], and microwave irradiation [12]. Generally, spinel-$Li_4Ti_5O_{12}$ is synthesized by a conventional solid-state reaction using TiO_2 and Li_2CO_3 (or LiOH) as starting materials at high temperatures [13] because solid-state reaction using Li and Ti source as raw materials is easy and economical.

Recently, $Li_4Ti_5O_{12}$, which has higher energy density than EDLC, has been studied for its potential as an anode material in an asymmetric hybrid supercapacitor. An asymmetric hybrid supercapacitor uses different materials with different operating potentials as cathode and anode materials, which can increase the overall cell potential, thereby resulting in higher energy and power densities [14]. Spinel-$Li_4Ti_5O_{12}$ has attracted attention as a superior electrode material for hybrid supercapacitor due to high energy density comparable with the secondary battery and highpower density of supercapacitors. However, research on $Li_4Ti_5O_{12}$ mainly focuses on anode material of rechargeable lithium ion batteries using $Li_4Ti_5O_{12}$. In this paper, we fabricate nanosized $Li_4Ti_5O_{12}$ particles via solid-state reaction and study electrochemical properties as anode material of the asymmetric hybrid supercapacitor.

2. Experimental

2.1 Sample synthesis and characterization

$Li_4Ti_5O_{12}$ was synthesized from TiO_2 and Li_2CO_3 as starting materials. Stoichiometric amounts of TiO_2 and Li_2CO_3 (Ti/Li = 5:4) were mixed in ethanol (99.9%). After

† Corresponding Author: SAMWHA CAPACITOR, Korea. (yoonjungrag@samwha.com)
* SAMWHA CAPACITOR, Korea. (wooxn@samwha.com)
Received: December 21, 2010; Accepted: June 13, 2011

ball milling for 12 h, the mixed slurry was oven-dried at 80℃. To obtain the final $Li_4Ti_5O_{12}$, the mixed precursors were heat-treated at 750, 800, 850, and 900℃ for 2 h under air atmosphere. The synthesized samples were characterized by X-ray diffraction (Riraku). XRD spectra were recorded with Cu Kα (λ = 1.5406 A°) radiation in the diffraction angle of 2θ from 10 to 80° at a scan rate of 5°min−1. BET surface area of $Li_4Ti_5O_{12}$ was determined by N_2 adsorption/desorption isotherms at 77 K (TriStar). The morphology and microstructure were observed using a scanning electron microscopy (Jeol).

2.2 Preparation of electrode films and electrochemical measurements

The electrodes of EDLC (negative and positive) and hybrid supercapacitor (positive electrode) were fabricated using activated carbon (BET: ~1700 m^2/g, ash contents <400 ppm, average particle size 10 ㎛). The negative electrodes of the hybrid supercapacitor were prepared by mixing $Li_4Ti_5O_{12}$ powder synthesized at 800℃, conductive carbon black (Super P), and polyvinylidene fluoride (PVdF) as a binder with the weight ratios 80:10:10. N-Methyl pyrrolidiznone (NMP) was used as a solvent. The slurry obtained from the mixture was coated by an aluminum current collector and dried at 150℃ to remove the NMP solvent. The electrode films of the EDLC were prepared by mixing activated carbon, conductive carbon black, and polytetrafluoroethylene (PTFE) as a binder in weight ratios 75:15:10. The electrode films were reserved in argon-filled dry box. The charge and discharge measurements were performed on a cylindrical cell (2245 size). The hybrid supercapacitor cell was assembled by using $Li_4Ti_5O_{12}$ as an anode and activated carbon (AC) as cathode. To compare the hybrid supercapacitor, EDLC cell was fabricated by using AC electrodes in the same way. The electrolyte was a 1 M solution of $LiPF_6$ in ethylene carbonate (EC)-dimethylcarbonate (DMC) 2:1 in v/v. Nonwoven fabric was used as the separator. The electrochemical performance was evaluated in the potential range of 2.0-3.0V at room temperature using a programmable multichannel battery tester (Arbin Instruments). The cyclic voltammograms of the EDLC and hybrid supercapacitor were characterized using a three-electrode cell. Voltage range of CVs was 0-3V, whereas the scan rate was 50 mVs−1.

3. Results and discussion

Fig. 1 shows the XRD patterns of the $Li_4Ti_5O_{12}$ powders. Small TiO_2 peaks were observed at 750℃ calcinations temperature. The XRD patterns show the difficulty of synthesizing pure $Li_4Ti_5O_{12}$ at 750℃ because of impurity phase rutile TiO_2. In contrast, the patterns of the samples synthesized at 800, 850, and 900℃ are closely in accordance with the $Li_4Ti_5O_{12}$ cubic spinel phase structure. The process exhibited diffraction peaks at 2θ (deg.) values around 18°, 35°, 37°, 43°, 49°, 58°, 63°, 66°, 75°, 76°, and 79°, which corresponds to (111), (311), (222), (400), (331), (511), (440), (531), (533), (622), and (444) planes, respectively. Because calcination temperature increases from 750℃ to 800-900℃, the crystallinity of $Li_4Ti_5O_{12}$ improved and the impurity phase TiO_2 was not detected. No obvious difference was found between the XRD patterns obtained at 800-900℃ for 2 h. The cell parameter of the $Li_4Ti_5O_{12}$ is 8.358 Å. The XRD patterns correlate with reports from previous studies [15]. The XRD results of the samples $Li_4Ti_5O_{12}$ obtained at 800, 850, and 900℃ for 2 h are well defined as single-phase $Li_4Ti_5O_{12}$, with cubic symmetry, space group Fd3m, which coincides with JCPDS data, Card No. 26-1198 [16]. Therefore, reaction between TiO_2 and Li_2CO_3 takes place at temperature higher than 750℃.

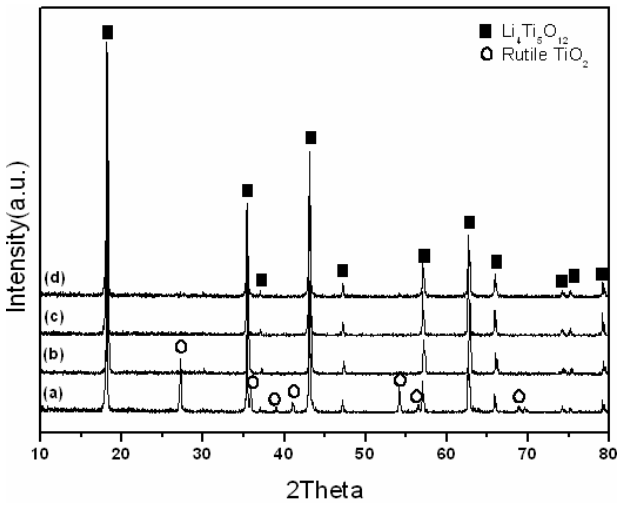

Fig. 1. XRD patterns of $Li_4Ti_5O_{12}$ after calcinations at (a) 750; (b) 800; (c) 850; (d) 900℃

Fig. 2 shows the SEM images of the $Li_4Ti_5O_{12}$ samples heat-treated at various temperatures for 2 h under air atmosphere. The process revealed that the particle size of sample calcined at 750℃ is smaller than other samples because perfect spinel crystal could not be formed. With increasing synthesis temperature, average particle diameter of the $Li_4Ti_5O_{12}$ was increased. The micrographs reveal that the morphology, surface area, and particle size were affected by synthesis temperature. The BET surface areas of the powders were measured to be 4.1 m^2/g (750℃), 3.8 m^2/g (800℃), 3.5 m^2/g (850℃), and 3.1 m^2/g (900℃), respectively. Grain growth occurs with the size increase of crystallites in materials at high temperature. Thus, the increase of synthesis temperature results in grain growth, as shown by Fig. 2.

Fig. 3 shows the discharge curves of the hybrid supercapacitor and EDLC (cut-off voltage 2.0V). Before charging, the cell potential was maintained at 0V for 5 min.

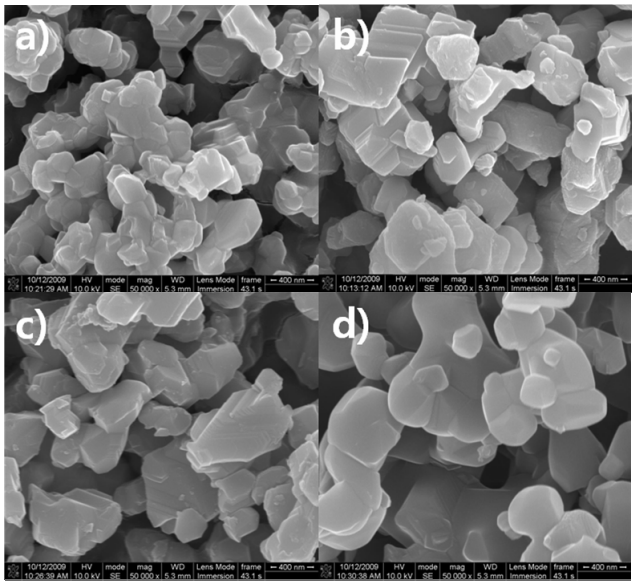

Fig. 2. SEM images of the $Li_4Ti_5O_{12}$ after calcination at (a) 750; (b) 800; (c) 850; (d) 900℃

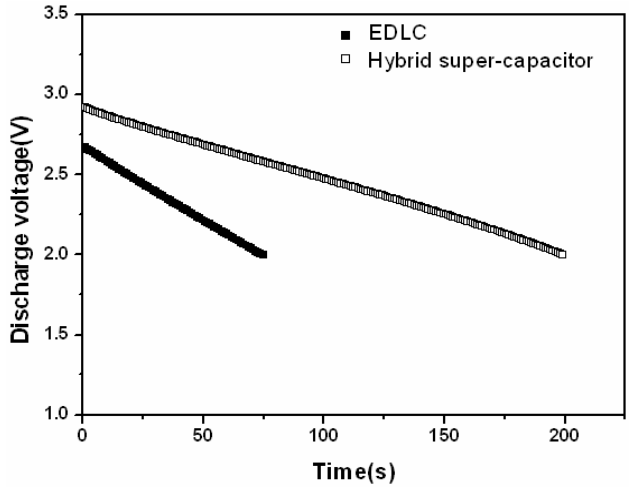

Fig. 3. Discharge curves of EDLC and hybrid super-capacitor

At the beginning of the discharge cycling, a potential drop was observed. The discharge curves were nearly linear. Capacitances were calculated from each discharge curve. The capacitance of EDLC was recorded at 109 F, whereas the hybrid supercapacitor was 209 F. Results show that energy density of the hybrid supercapacitor is higher than EDLC, whereas its power density is worse. The differences of the specific capacity and discharge time between the hybrid supercapacitor and EDLC show that the hybrid supercapacitor system ($AC/Li_4Ti_5O_{12}$) is composed of the capacitor system and the secondary battery system, as described in the following equations

$$AC + PF_6^- \leftrightarrow AC^+ \bullet PF_6^- + e^- \quad \text{[Cathode]}$$
$$Li_4Ti_5O_{12} + 3Li^+ + 3e^- \leftrightarrow Li_7Ti_5O_{12} \quad \text{[Anode]}$$

The $Li_4Ti_5O_{12}$ electrode exhibits oxidation-reduction behavior. However, the activated carbon electrode exhibits a double-layer electric behavior attributed to the electrostatic adsorbing–desorbing process of PF_6^- on AC. Figs. 4a and 4b show the obvious different electrochemical behaviors of EDLC and hybrid supercapacitor. The asymmetric hybrid supercapacitor is presented where the cathode (AC) stores charge through a double layer of electric anions on the surface of an AC. Anode ($Li_4Ti_5O_{12}$) is a crystalline intercalation compound, which supports the fast reversible intercalation of lithium ions [17].

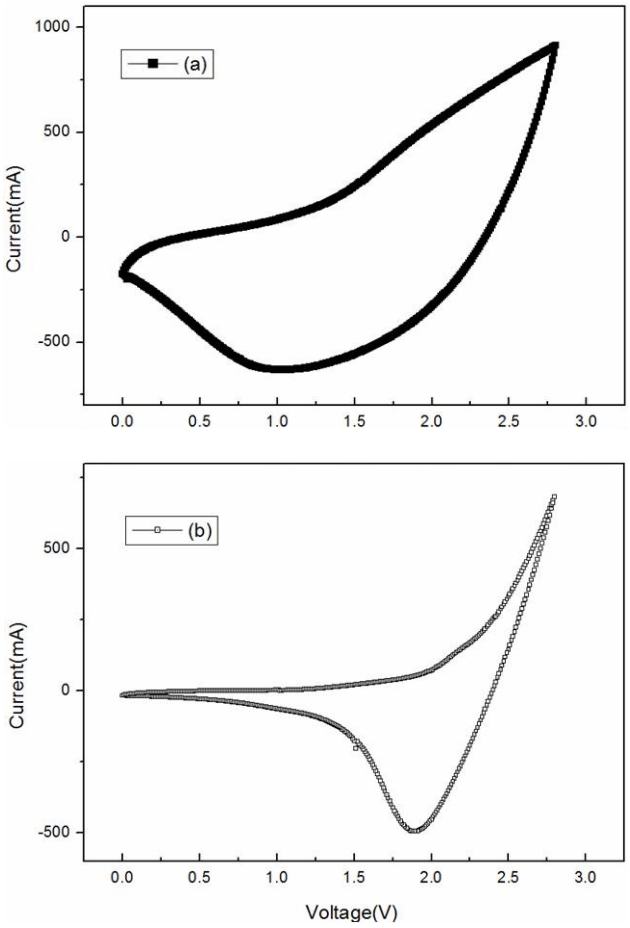

Fig. 4. CV's of EDLC AC/AC (a) and the hybrid supercapacitor $AC/Li_4Ti_5O_{12}$ (b)

Fig. 5 shows cycle performances of the hybrid supercapacitor and EDLC. After 10,000 cycles, capacitance losses of the hybrid supercapacitor and EDLC are 22.1% and 11.4%, respectively. Results indicate that the cycle performance of hybrid supercapacitor is worse than that of EDLC when the same cathode is used in these cells. However, the capacitance of hybrid supercapacitor is 175 F at 1st cycle and 119 F at 10,000th cycle, which is higher than that of EDLC. This finding indicates that the energy storage performance of hybrid supercapacitor is better than that of EDLC. These facts illustrate that $Li_4Ti_5O_{12}$ as an anode enhances the capacity of the capacitor.

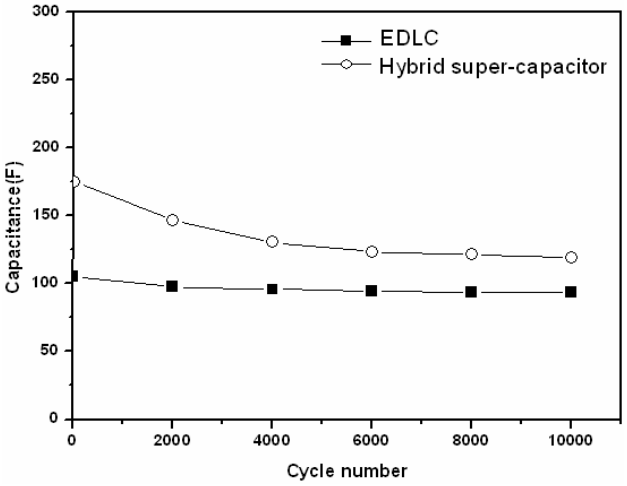

Fig. 5. Cycle performance of the hybrid supercapacitor and EDLC cycled at 3 A

Fig. 6 shows the discharge curves of the hybrid supercapacitor and EDLC at different discharge current rates for rate capability. The current charge and discharge rates are the same for each case. Fig. 6 also shows that the capacitances of all samples decrease with increasing current rate discharge because of polarization. The capacitance of the hybrid supercapacitor decreases from 209 to 101 F after 20 cycles when discharged at several specific current densities ranging from 1 to 10 A. The capacitance of the EDLC decreases only slightly after 20 cycles. These results demonstrate good EDLC performance of high charge-discharge rates in comparison with the hybrid supercapacitor because its power density is better than that of the hybrid supercapacitor.

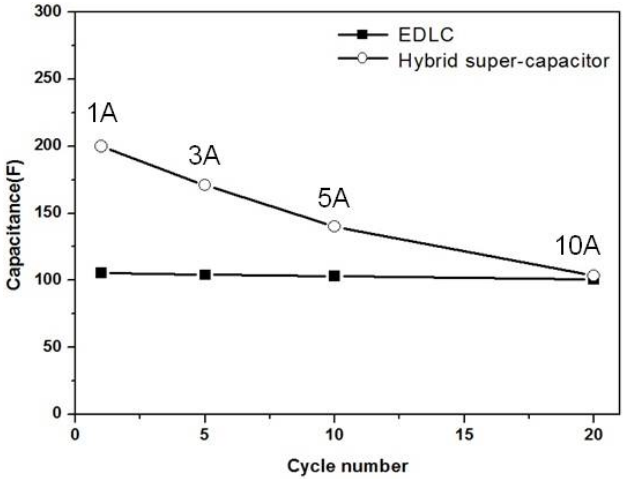

Fig. 6. Specific capacitances of the hybrid supercapacitor and EDLC at different current rates

4. Conclusion

In this work, we synthesized $Li_4Ti_5O_{12}$ powders by using conventional solid-state reaction. Single phase $Li_4Ti_5O_{12}$ was synthesized when the calcinations temperature was higher than 800℃. The hybrid supercapacitor with $Li_4Ti_5O_{12}$ anode was fabricated afterwards to form the AC/$Li_4Ti_5O_{12}$. The hybrid supercapacitor was composed of the capacitor system (cathode) and the lithium ion secondary battery system (anode). The hybrid supercapacitor utilizing $Li_4Ti_5O_{12}$ as an anode exhibits high capacitance compared to EDLC because of electrochemical process with intercalation/de intercalation of lithium into the spinel-$Li_4Ti_5O_{12}$. When the hybrid supercapacitor and EDLC were discharged at 1 A, capacitance of the hybrid supercapacitor was recorded at 209 F, which outperforms EDLC by approximately two times. Results show that the hybrid supercapacitor has the advantages of both the high rate capability of the EDLC and the high capacity of the lithium ion secondary battery.

References

[1] Y. J. Lee, S. Y. Park, J. G. Seo, J. R. Yoon, J. H. Yi, I. K. Song, Curr. App. Phys. vol. 11, pp. 631-635, 2011.
[2] Y. F. Tang, L. Yang, Z. Qiu, J. S. Huang, Electrochem. Commun. Vol. 10, pp. 1513-1516, 2008.
[3] T. Ohzuku, A. Ueda, N. Yamamoto, J. Electrochem. Soc. vol. 142, pp. 1431-1435, 1995.
[4] K. Zaghib, M. Armand, M. Gauthier, J. Electrochem. Soc. vol. 145, pp. 3135, 1998.
[5] K. Zaghib, M. Simoneau, M. Armand, M. Gauthier, J. Power Sources, vol. 81-82, pp. 300-305, 1999.
[6] M. Venkateswarlu, C. H. Chen, J. S. Do, C. W. Lin, T. C. Chou, B. J. Hwang, J. Power Sources, vol. 146, pp. 204-208, 2005.
[7] J. Gao, C. Y. Jiang, J. R. Ying, C. R. Wan, J. Power Sources, vol. 155, pp. 364-367, 2006.
[8] Y. J. Hao, Q. Y. Lai, J. Z. Lu, H. L. Wang, Y. D. Chen, X. Y. Ji, J. Power Sources, vol. 158, pp. 1358-1364, 2006.
[9] J. R. Li, Z. L. Tang, Z. T. Zhang, Electrochem. Commun. Vol. 7, pp, 894, 2005.
[10] D. Takayuki, I. Yasutoshi, A. Takeshi, O. Zempachi, Chem. Mater. vol. 17, pp. 1580-1582, 2005.
[11] Y. Bai, F. Wang, F. Wu, C. Wu, L. Y. Bao, Electrochim. Acta, vol. 54, pp. 322-327, 2008.
[12] J. Li, Y. L. Jin, X. G. Zhang, H. Yang, Solid State Ionics, vol. 178, pp. 1590-1594, 2007.
[13] K. Zaghib, M. Simoneau, M. Armand, M. Gauthier, J. Power Sources, vol. 81-82, pp 300-305, 1999.
[14] M. S. Hong, S. H. Lee, S. W. Kim, Electrochem. Solid St. vol. 5, pp. A227-A230, 2002.
[15] E. M. Sorensen, S. J. Barry, H. K. Jung, J. R. Rondinelli, J. T. Vaughey, K. R. Poeppelmeier, Chem. Mater. Vol. 18, pp. 482-489, 2006.
[16] S. Y. Yina, L. Songb, X. Y. Wanga, M. F. Zhanga, K.

L. Zhanga,c, Y. X. Zhanga, Electrochimica Acta, vol. 54, pp. 5629-5633, 2009.
[17] J. R. Yoon, K. M. Lee, and S. W. Lee, Trans. EEM 10 (1) 5, pp. 5-8, 2009.

Byung Gwan Lee was born in Kyunggi-do, Korea. He received his B.S. and M.S. degrees in Advanced Material Engineering from Kookmin University, Seoul, Korea, in 2007 and 2009, respectively. He currently works as a Researcher for Samwha Capacitor Co. Ltd.

Jung Rag Yoon was born in Kangwon-do, Korea. He received his BS, MS, and Ph.D degrees in Electrical Engineering from Myoung Ji University, Korea in 2001, 2003, and 2009, respectively. Currently, he serves as an R&D Center Manager for Samwha Capacitor Co. Ltd.